Calibration and Sensitivity Analysis of Upper Level VSC-HVDC Controls

Luigi Vanfretti
School of Electrical Engineering
Royal Institute of Technology (KTH)
Stockholm, Sweden.
luigiv@kth.se

Mohammed Ahsan Adib Murad
School of Electrical & Electronic Engineering
University College Dublin (UCD)
Dublin, Ireland.
mohammed.murad@ucdconnect.ie

Francisco Jóse Gómez-López
School of Electrical Engineering
Royal Institute of Technology (KTH)
Stockholm, Sweden.
fragom@kth.se

***Abstract*—High Voltage Direct Current (HVDC) interconnections have seen an increased rate of deployment, in particular to exploit distant renewable energy sources. In order to design and understand their behavior, including their effect on the overall network, different computer tools are used for modeling and simulation. This approach results in several challenges in modeling and simulation consistency, particularly for HVDC systems. In this paper, to address some of these issues, the standardized Modelica modeling language is used to model a VSC (Voltage Source Converter)-based HVDC and its upper-level controllers, suitable for dynamic analyses. The use of Modelica-tools that support the FMI standard for model-exchange allows to utilize the model in different environments. In this work, the FMI standard is used to import the VSC-HVDC model into the RaPId toolbox environment, thus allowing to calibrate the VSC-HVDC phasor model against reference waveform generated from its corresponding EMTP-RV model. Model calibration is carried out through parameter identification and a sensitivity analysis is carried out to interpret the identification results.**

***Index Terms*—EMTP, HVDC, System Identification, VSC, Modelica.**

I. Introduction

A. Motivation

High Voltage Direct Current (HVDC) transmission systems have received renewed attention in the last decade due to their applications for long distance power transmission, particularly for off-shore wind interconnections [1]. Two main converter technologies for HVDC are the Line-Commutated Converter (LCC) and Voltage Source Converter (VSC), which are used for different applications in power systems [2]. VSC-based HVDC systems provide certain advantages w.r.t. LCC, including independent control of active and reactive power, and others [3]. An overview of different VSC topologies are reported in [4] and includes conventional two-level, multi-level diode-clamped, floating capacitor multi-level converters, among others. Recently, the Modular Multilevel Converter (MMC) technology has been adopted because of its advantages w.r.t. other multilevel converter topologies for HVDC applications [5].

This work was supported in part by the FP7 iTesla project, the ITEA3 openCPS project, and STandUP for Energy. Mohammed Ahsan Adib Murad is supported by Science Foundation Ireland under Grant No. SFI/15/IA/3074.

With the adoption of different types of HVDC technologies, modeling and simulation of these devices has become of crucial importance for different network studies, and of particular interest in the context of this work, for dynamic security assessment. An overview of these models for transient simulation is given in [6]. One of the iTesla project [7] Transmission System Operators (TSOs) had available an HVDC-VSC model that is used for electromagnetic transient simulations, and its been implemented using EMTP-RV [8]. This model can only be used in the EMTP-RV software, however dynamic security assessment carried out using the iTesla toolbox [9], requires phasor time-domain models that can be used by different simulation engines (e.g. Eurostag, PSS/E, OpenModelica and/or Dymola for Modelica models). Hence, the development of a VSC-HVDC model available for phasor time-domain simulation using a Modelica-compliant simulation engine was necessary for the iTesla toolbox internal simulation, data management, and model exchange needs. In addition, the Modelica model needs to be parametrized adequately so that the model can represent the same behaviour as the EMTP-RV model and also when used to model an actual VSC-HVDC link. Traditionally power system simulation software packages address forward problems, i.e. if a model is provided with known set of parameters, the trajectories can be determined. However, addressing inverse problems, e.g. if trajectories can be measured from actual system, the parameters can be estimated [10], is also crucial. Using the RaPId parameter identification toolbox, such inverse problems can be solved [11].

Modelica [12], is an object oriented equation-based standardized language suitable for modeling complex cyber-physical systems. Among its advantages, it is worth to mention that it has a large standardized library of component models from different domains (e.g. electrical, mechanical, thermal, fluid etc) and it supports acausal modeling. In addition, several Modelica tools also support the FMI standard for model exchange and co-simulation, which has been accepted by a large user community and it is being used for a great number of applications [13]. Due to this and several other unique advantages, the iTesla project choose Modelica as the main modeling language to represent power system dynamic models.

B. Previous Work

There are already two implementations of VSC-HVDC models using Modelica in [14] and [15] however, these have not been validated against a high bandwidth model (EMT type model). In addition, these specify the inner control, phase lock loop (PLL) and modulation strategy, which are unnecessary for large scale stability studies, as such detailed representation leads to an increase in computational requirements and simulation execution time.

C. Paper Contributions

This paper presents a Modelica VSC-HVDC model that has gone through a software to software (SW-to-SW) validation against EMTP-RV, and can be used for phasor time domain simulations and model exchange [16]. Herein, the calibration of the Modelica VSC-HVDC model w.r.t. reference signals from the simulation of its corresponding EMTP-RV model is carried out. While previous work [17] has considered the identification of simplified VSC models represented with equivalent open loop transfer functions, this work differs in that it provides methods to calibrate the controllers parameters by minimizing the error of the full non-linear model response while utilizing real or synthetic time-series data. However, measurement data was not available to carry out this work, and thus, simulation results of EMTP-RV are used as synthetic measurement data.

The remainder of this paper is organized as follows. Section II describes the basic principles underlying the model implementation in Modelica and EMTP-RV. In Section III, the identification process is described, while in Section IV a sensitivity analysis is carried out. Finally, in Section V, conclusions are drawn.

II. VSC-HVDC Models

In EMTP-RV two types of VSC-based MMC station models are available: Monopole and Bipole configuration with ground return. The MMC stations are represented using four kinds of models: (a) Full detailed model, (b) Detailed equivalent model, (c) Switching function of arm model, and (d) Average-value model (AVM). The three-phase configuration of the MMC topology is shown in Fig. 1.

In this work the AVM model with an upper level control system is implemented. The full description of the model is documented in [18]. In this Section, the most relevant components of the model available in EMTP-RV are reviewed, as they are replicated in the Modelica implementation.

A. Average-Value Model (AVM)

In an AVM, the power electronic switches (IGBTs) and diodes are not modeled in detail, instead, the MMC behavior is represented using controlled voltage and current sources. Thus, an ideal behavior of the internal variables of the MMC is assumed. For each phase $j = a, b, c$; the voltage of the converter is derived from Fig. 1,

$$v_{conv_j} = \frac{L_{arm}}{2}\frac{di_j}{dt} - v_j \tag{1}$$

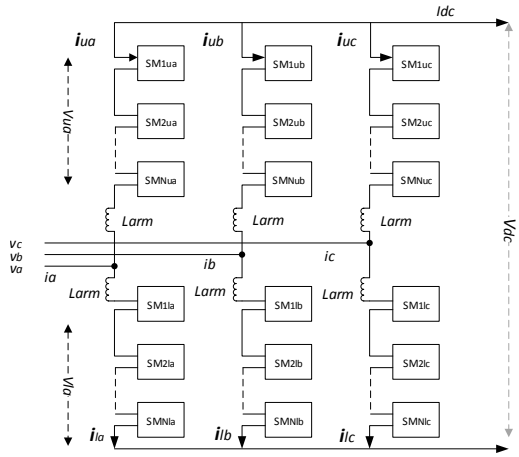

Fig. 1. MMC topology.

where, L_{arm} is the arm inductance. Assuming the total number of sub-modules in each phase is constant,

$$v_{u_j} + v_{l_j} = V_{dc} \tag{2}$$

where, v_{u_j} and v_{l_j} are upper and lower arm voltages. Using (1) and (2) the MMC is represented as a classical VSC. The controlled voltage source in the AC side is determined by:

$$v_{conv_j} = v_{ref_j}\frac{V_{dc}}{2} \tag{3}$$

where, v_{ref_j} are the reference voltages generated from the inner controller of the upper level control. Based on the power balance principle, the DC side model equations are derived assuming no energy is stored inside the MMC converter, as follows

$$V_{dc}I_{dc} = \sum_{j=a,b,c} v_{conv_j} i_j \tag{4}$$

from where the DC side current is given by,

$$I_{dc} = \frac{1}{2}\sum_{j=a,b,c} v_{ref_j} i_j \tag{5}$$

Using the principles above, the AVM model implementation in EMTP-RV allows to build up an entire VSC-HVDC model. The AC side voltage for each phase is calculated using (3) and the DC side current I_{dc} is calculated using (5).

B. Control System

1) Control System Hierarchy: The VSC type MMC topology uses an upper level control system, which includes outer and inner controllers. The upper level control system serves two main purposes: (i) to regulate system variables, i.e. the active and/or reactive power or voltages, and (ii) to generate reference voltages, which are used as input to the AVM.

2) Upper Level Control: The VSC-MMC model uses the classical vector control strategy. The inputs to the upper level control are three phase p.u. variables, using the matrix (6) these variables are converted to two quadrature axis components rotating at synchronous speed ($\frac{d\theta}{dt}$). The phase angle θ is

calculated using a Phase-Locked Loop (PLL). The Clarke transformation, P/Q/VAC calculations and dq transformation are implemented in EMTP-RV to compute the variables required for the outer and inner controllers.

$$T = \frac{2}{3}\begin{bmatrix} cos(\omega t) & cos(\omega t - \frac{2\pi}{3}) & cos(\omega t + \frac{2\pi}{3}) \\ -sin(\omega t) & -sin(\omega t - \frac{2\pi}{3}) & -sin(\omega t + \frac{2\pi}{3}) \\ \frac{1}{2} & \frac{1}{2} & \frac{1}{2} \end{bmatrix} \quad (6)$$

The dq transformed voltage and currents are calculated using the transformation matrix T,

$$i_{dq} = T i_{abc} \quad (7)$$

$$v_{dq} = T v_{abc\_grid} \quad (8)$$

The AC grid voltage, active and reactive power are calculated from the dq reference,

$$P = v_d i_d + v_q i_q \quad (9)$$

$$Q = -v_d i_q + v_q i_d \quad (10)$$

$$v_{grid} = \sqrt{v_d^2 + v_q^2} \quad (11)$$

The signals are converted to per unit (p.u.) quantities before entering the upper level control system. The outer and inner control block is used to control active power, reactive power, DC and AC voltage. All the control is achieved using proportional and integral (PI) controllers. Finally, the dq to abc transformation is used to convert the dq reference to three phase voltage references.

C. VSC Model Implementation in Modelica

An equivalent AVM model of the VSC converter is implemented in Modelica, including the upper level controller. In Modelica, the AC-side of the converter is a current injector and the DC-side is a current source, shown in Fig 2. All the controls implemented in Modelica are the same as the upper level controllers in EMTP-RV. The inputs of the upper level controls in Modelica are Vdc, P, Q, Vac measured at the DC or AC side of the physical model. The outputs of the upper level controls in Modelica are named Irorder, Iiorder. These are the real and imaginary currents injected into the AC side of the grid. Inner controllers, are not of interest in the context of this work because phasor models without detailed modeling of the power electronic stage was considered to be sufficient to meet accuracy needs and simpler to satisfy simulation requirements.

Remarks:

- In the Modelica model it is not necessary to calculate the dq references because the phasor modeling considers only positive sequence voltage and currents.
- The active power, reactive power, and AC voltage in the Modelica model are calculated using real and imaginary current and voltages.

The software-to-software validation of the Modelica model against its EMTP-RV reference is presented in [16].

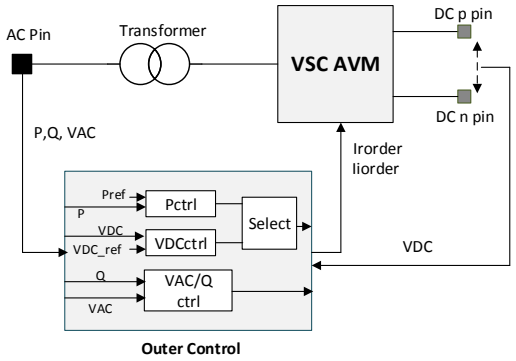

Fig. 2. Modelica implementation of VSC converter.

III. Parameter Calibration Using RaPId

A. RaPId's Workflow

Using the RaPId toolbox, parameters can be identified for any Modelica model by generating an FMI standard-compliant Flexible Mockup Unit (FMU). As illustrated in Fig. 3 , RaPId takes the FMU with the system model and measurement data as input, and then simulates the model using a set of initial 'guess' parameters. Then the adequacy of the parameters is assessed by evaluating an objective function that quantitatively appraises the error criteria between the simulation results and the measurement data. This process continues sequentially until an optimization method[1] finds a set of parameters satisfying the error criteria or when the maximum number of simulations is reached. The initial parameter values and bounds can be set by the user.

B. Proposed Identification Procedures

Two different procedures for parameter identification using RaPId are considered. The first approach considered each controller individually, while the second approach considered

[1]RaPId has several native optimization algorithms, and also includes those available in the Optimization Toolbox and Global Optimization Toolbox for MATLAB. RaPId can be configured to use external optimization packages, provided that the software provides a native interface to link it to MATLAB. Hence, RaPId is agnostic and flexible to the choice of optimizer selected by the user, see: https://github.com/SmarTS-Lab/iTesla_RaPId

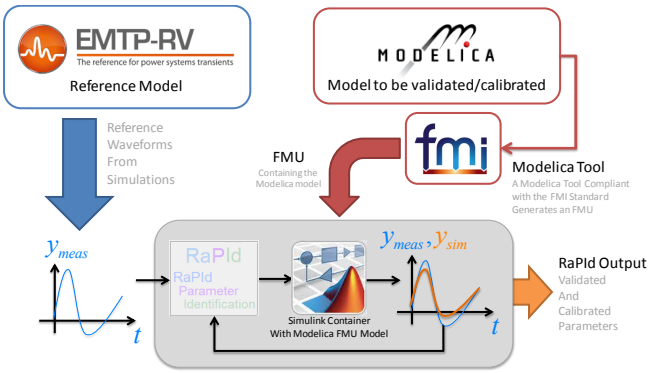

Fig. 3. RaPId's work-flow

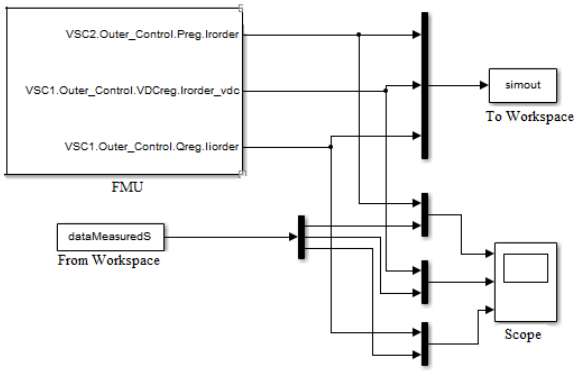

Fig. 4. Simulink container used for parameter identification in RaPId.

of all controllers simultaneously. In this paper only the simultaneous calibration results are presented, while [16] both approaches are compared.

Before generating an FMU for calibration using RaPId, 'test values' (uncalibrated parameters that are different from those in EMTP-RV) were provided to the Modelica model. In addition, the initial guess and bounds of the parameters values are given to RaPId's optimizer. Observe that these start initial guess values are also different from those used in EMTP-RV. The parameter settings and original values used in EMTP-RV are given in Table I and the simulink container used in RaPId is shown in Fig 4.

TABLE I
INITIAL PARAMETER VALUES AND SETTINGS USED IN RAPID

Parameters	EMTP vaule	Initial guess	Minimum	Maximum
Pctrl_Ki (VSC2)	30	25	5	50
Pctrl_Kp (VSC2)	0	5	0	10
Qctrl_Ki (VSC1)	30	25	10	50
Qctrl_Kp (VSC1)	0	5	0	10
VdcCtrl_Kp (VSC1)	24	20	10	40
VdcCtrl_Ki (VSC1)	734.7	750	550	950

C. Simultaneous Identification of all Parameters

The simultaneous identification process takes into account the identification of all the specified controller parameters within the same model. This implies that three controller outputs were measured and compared simultaneously. The identification process was carried out in six experiments with different ramp and step perturbations. In each experiment 1000 iterations (work-flow executions) are considered. Statistical analysis of the identified parameters in each experiment using RaPId was carried out. The mean (μ), standard deviation (σ), variance (σ^2) and confidence interval (95%) of all the parameters identified are summarized in Table II. Using the resulting lower and upper bounds of the confidence intervals, simulations are carried out again by applying different perturbations, as shown in Fig. 5. The Fig. 5 also shows the simulation results obtained when using test values (for illustration purposes). In addition to these statistical results, quantitative assessment of the simulation results shown in Fig.

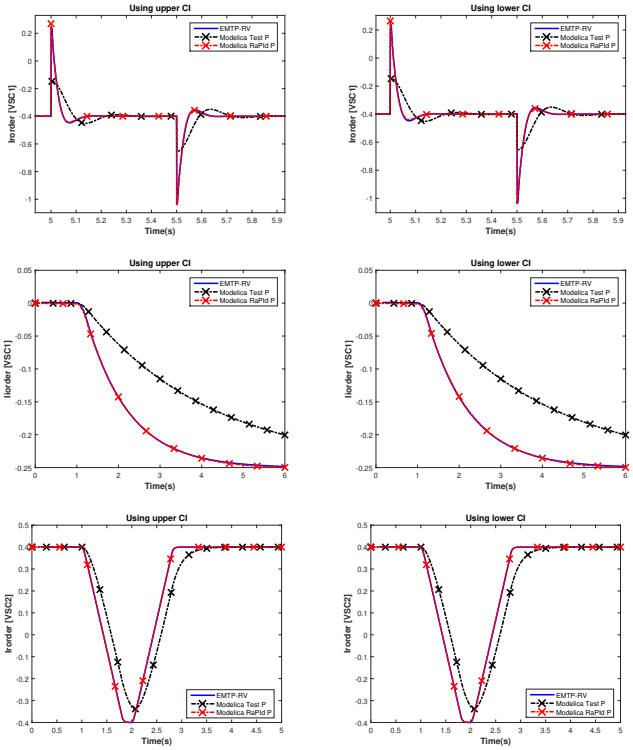

Fig. 5. Simulation results using the parameter values at 95% confidence interval bounds and test values. Blue traces (synthetic measurements from EMTP-RV), red traces (simulation using the parameters from the CI bounds), black traces (test value uncalibrated).

5 is carried out using the Root Mean Square Error (RMSE). All the RMS errors are given in Table III.

As shown by the results discussed above, the identification processes provides adequate estimates for the active power and Q/VAC controller gain parameters. However, the integral gain parameter of the VDC controller is identified with high variance and a broad confidence interval, and the validity of the estimates requires further analysis as discussed next.

IV. SENSITIVITY ANALYSIS

The high variance shown in the estimation process of the VDC controller integral gain parameter (VdcCtrl_Ki) can be interpreted as either an indicator of (i) the poor quality of the parameter estimate (and implicitly the estimation process), or (ii) of the modeling adequacy. Hypothesis (i) can be discarded by virtue of the consistent identification results obtained for all other parameters and control loops. To be able to prove hypothesis (ii) and determine the source of the high variance in the identification results of VdcCtrl_Ki, two different sensitivity analyses on the DC voltage controller are performed and described in the following sections.

A. Linear Analysis

The system's closed-loop eigenvalues are obtained by independently varying the parameters of each controller and linearizing the entire model using Modelica. Ten equidistant points of each gain value are considered within the same range used in the identification process (see Table I). Results are

TABLE II
PARAMETER IDENTIFICATION RESULTS

	Pctrl_Ki (VSC2)	Pctrl_Kp (VSC2)	Qctrl_Ki (VSC1)	Qctrl_Kp (VSC1)	VdcCtrl_Kp (VSC1)	VdcCtrl_Ki (VSC1)
μ	31.53	0	29.32	0.263	26.66	834.19
σ	0.072	0	0.082	0.046	0.083	37.501
σ^2	0.005	0	0.006	0.002	0.007	1406.4
CI (95%)	31.45 31.60	0	29.23 29.40	0.21 0.31	26.58 26.75	794.83 873.54

TABLE III
QUANTITATIVE ASSESSMENT (RMSE)

Variable	Upper CI	Lower CI	EMTP-RV value	Test Value
Irorder (VSC2)	1.8283e-04	1.8954e-04	9.3324e-4	0.0813
Iiorder (VSC1)	0.0011	0.0011	0.0016	0.0687
Irorder (VSC1)	0.0050	0.0049	0.0049	0.0252

summarized for the most relevant eigenvalue in Fig. 6 and Table IV. In Fig. 6, the root loci for the parameter changes of VDC and P controllers is shown. For the VdcCtrl_Kp parameter, the complex-pair of eigenvalues move widely along the left half plane, while for VdcCtrl_Ki parameter the eigenvalues have a very narrow sweep in the $\Re$-axis and a relatively broader reach in the $\Im$-axis. In contrast, the corresponding loci for the P controller gain parameters sweeps on the negative $\Re$-axis, as expected. As it can be observed in Table IV, the bandwidth of VdcCtrl_Kp ranges from [0 6.53] Hz while that of VdcCtrl_Ki is [3.458 6.114], implying that VdcCtrl_Kp overlaps the bandwidth of VdcCtrl_Ki. Given this overlap and the large damping effect of the proportional gain (with damping $>$ 50% at VdcCtrl_Kp $\geq$ 20), the effect of VdcCtrl_Kp is to dominate the control's loop response. This is the implication of the wide sweep of the VdcCtrl_Kp loci in Fig. 6. As a result, during the calibration process, VdcCtrl_Kp will quickly converge to the actual parameter, while VdcCtrl_Ki will take an arbitrary value within the loci in Fig. 6 as it does not influence the control loop response and consequently this does not reflect in the objective function being minimized (error).

B. Non-linear Analysis

To identify the sensitivity of control loop associated with the VdcCtrl_Ki parameter, non-linear time-domain simulations are carried out while applying a step change from 1 to 1.019 at the VDC reference in both Modelica and EMTP-RV. Different values for VdcCtrl_Ki=[250 1500] are used in each new simulation. A plot of the RMS errors (i.e. EMTP-RV vs. Modelica) of the output of the VDC controller versus the parameter VdcCtrl_Ki is shown in Fig. 7. From the figure, the RMS errors are [0.0089 0.0069] for VdcCtrl_Ki=[250 1500], and stagnates at 0.0033 for VdcCtrl_Ki=[780 850]. This indicates that the variation of VdcCtrl_Ki has a negligible impact in the output of the controller for the type of perturbation analyzed (i.e. small-perturbation).

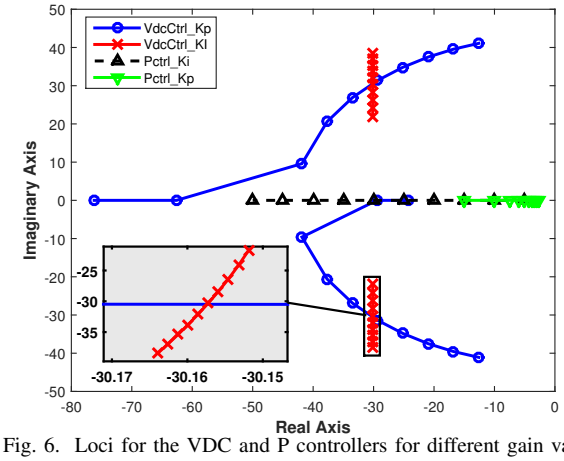

Fig. 6. Loci for the VDC and P controllers for different gain values.

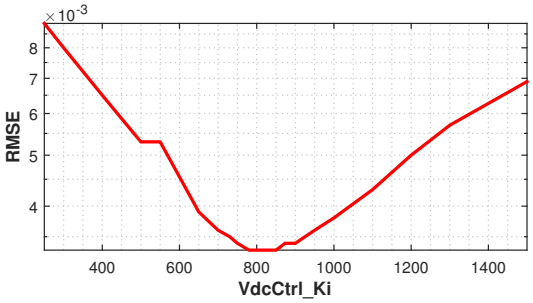

Fig. 7. RMS error with VdcCtrl_Ki range [250, 1500].

V. CONCLUSION

This paper presented a Modelica implementation of a VSC-HVDC model that is capable of providing the same simulation results as its EMTP-RV reference model when switching controls are not included. This allows the model to be used in large-scale simulations with a high degree of confidence. Before the model can be used for this purpose, it needs to be parametrized appropriately. To achieve this, a parameter estimation approach using FMUs from the Modelica model and the RaPId toolbox was presented. The identification process successfully identified all the controls' gain parameters with low variance and the 95% confidence interval, except for the integral gain of the DC controller VdcCtrl_Ki. From the results of the sensitivity analysis in Section IV it can be concluded that VdcCtrl_Ki does not have a significant impact from small-signal stability point of view, as the proportional gain (VdcCtrl_Kp) dominates the control loop. This was confirmed through non-linear analysis of small perturbations at the reference of the controller. Hence, the results from the identification process are consistent with the sensitivity

TABLE IV
CLOSED-LOOP EIGENVALUES FOR THE VDC CONTROLLER AT DIFFERENT GAINS

VdcCtrl_Kp	10	13.3	16.6	20	23.3	26.6	30	33.3	36.6	40
Eigenvalue (3&4)	-12.58 ±41.08	-16.77 ±39.55	-20.95 ±37.50	-25.14 ±34.83	-29.32 ±31.39	-33.50 ±26.87	-37.67 ±20.61	-41.85 ±9.60	-29.44 & -62.60	-24.18 & -76.21
Damping (%)	29.29	39.03	48.78	58.52	68.26	77.99	87.73	97.46	100	100
Oscillation F(Hz)	6.53	6.29	5.96	5.54	4.99	4.27	3.28	1.52	0	0
VdcCtrl_Ki	550	594.4	638.8	683.3	727.7	772.2	816.6	861.1	905.5	950
Eigenvalue (3&4)	-30.151 ±21.72	-30.153 ±24.15	-30.154 ±26.36	-30.155 ±28.40	-30.157 ±30.30	-30.158 ±32.08	-30.159 ±33.78	-30.16 ±35.39	-30.162 ±36.93	-30.16 ±38.41
Damping (%)	81.13	78.04	75.28	72.79	70.54	68.48	66.59	64.85	63.24	61.75
Oscillation F(Hz)	3.458	3.844	4.196	4.520	4.822	5.107	5.376	5.633	5.878	6.114

analysis, and explain the large variance for the integral gain.

The analyses above do not imply that the integral gain parameter (and related confidence interval) are invalid. In fact, what the results show is that the value for the parameter can be chosen arbitrarily from the confidence interval when considering small perturbations. The second hypothesis in Section IV raised the question of modeling adequacy. Indeed, the effect of VdcCtrl_Ki is negligible for small perturbations because DC-voltage control loop the internal capacitor dynamics already provide the integral action that reduce the steady-state error of the loop - this is a "natural" integral effect. The commonly used PI control law at the VDC controller assumes that the corresponding active power controller at the other converter is sufficiently fast [20], which is the case in this work. This should also be kept in mind because the DC voltage control loop is implemented as an additional high level controller that modifies the active power control output that is fed to the low level controller as a reference signal ([19], see Chapter 2).

The conclusion is that as a fast response is obtained by using the AVM model, when performing calibration of this controller gain, the capacitor dynamics overtake the control action that could be provided by the integral controller. In practice, the integral parameter is included in high level control design to reduce steady-state errors more quickly in the presence of disturbances. However, to accurately include this during the high level control analysis, this would require a more detailed model of the VSC that can represent, with a higher fidelity, the aggregate arm fast-dynamics. During the design of the low level controls and power electronic components, the PI controller is actually replaced with a two degree-of-freedom controller (a lead-lag controller), known as a pre-filter, and the equivalent arm capacitance must be designed accordingly (see [20], Chapter 5). Thus, by developing a better representation of this behavior of the VSC to be used in high level control analysis (i.e. without the need of simulating the internal modulation and switching of IGBTs) and by instead replacing the PI loop with a lead-lag controller, the calibration (or design) for this control loop could to be carried out using non-linear methods for which the RaPId toolbox is well suited. This will be pursued in further work.

REFERENCES

[1] M. P. Bahrman, "HVDC transmission overview," in *IEEE/PES Transmission and Distribution Conference and Exposition*, Chicago, IL, 2008, pp. 1-7

[2] E. N. Abildgaard and M. Molinas, "Modelling and control of the Modular Multilevel Converter (MMC)", *Energy Procedia*, Volume 20, 2012, Pages 227-236, ISSN 1876-6102.

[3] N. Flourentzou, V. G. Agelidis, and G. D. Demetriades, "VSC-based HVDC power transmission systems: An overview," *IEEE Trans. Power Electronics.*, vol. 24, no. 3, pp. 592-602, Mar. 2009.

[4] B. R. Andersen, L. Xu and K. T. G. Wong, "Topologies for VSC transmission," *Seventh International Conference on AC-DC Power Transmission*, pp. 298-304, 2001.

[5] A. Lesnicar, and R. Marquardt, "An innovative Modular Multilevel Converter Topology suitable for a wide power range, in *Proc. IEEE Power Tech. Conference*, vol. 3, Bologna, Jun. 2003.

[6] J. A. Martinez-Velasco, "Simulation of transients for VSC-HVDC transmission systems based on Modular Multilevel Converters," in *Transient Analysis of Power Systems:Solution Techniques, Tools and Applications*, 1, Wiley-IEEE Press, 2014, pp.648.

[7] iTesla: Innovative Tools for Electrical System Security within Large Areas. [Online] http://www.itesla-project.eu/

[8] EMTP-RV. [Online] http://emtp-software.com/

[9] L.Vanfretti, M.A.A. Murad, F.J. Gómez, G. Leon, S. Machado, J.B. Heyberger, S. Petitrenaud, "Towards automated power system model transformation for multi TSO phasor time domain simulations, *IEEE PES ISGT Europe*, Oct 9-12, 2016, Ljubljana.

[10] I. A. Hiskens, "Power system modeling for inverse problems," in *IEEE Transactions on Circuits and Systems I: Regular Papers*, vol. 51, no. 3, pp. 539-551, March 2004.

[11] L. Vanfretti, M. Baudette, A. Amazouz, T. Bogodorova, T. Rabuzin, J. Lavenius, F.J. Gómez-López, "RaPId: A modular and extensible toolbox for parameter estimation of Modelica and FMI compliant models", *SoftwareX*, Available online 25 August 2016, ISSN 2352-7110.

[12] Modelica and the Modelica Association. [Online] http://www.modelica.org/

[13] P. Fritzon, "Principles of object-oriented modeling and simulation with Modelcia 3.3: A cyber-physical approach", Wiley-IEEE Press, 2nd Edition, April, 2015.

[14] R. Majumder, B. Berggren and M. Larsson, "Development and comparison of DC grid model in PowerFactory and Dymola for controller design," in *IEEE Power& Energy Society General Meeting*, Vancouver, 2013, pp. 1-5.

[15] A. Olenmark, J. Sloth, A. Johnsson, C. Wilhelmsson, J. Svensson, "Control development and Modeling for flexible DC grids in Modelica", in *The 11th International Modelica Conference 2015*, France, September 21-23, 2015.

[16] L. Vanfretti, M.A. A. Murad and F.J. Gómez-López, "Calibrating a VSC-HVDC model for dynamic simulations using RaPId and EMTP simulation data," *IEEE PES General Meeting 2017*, Chicago, IL, 2017.

[17] L. Xu and L. Fan,"System identification based VSC-HVDC DC voltage controller design," *North American Power Symposium (NAPS)*, 2012, Champaign, IL, 2012, pp. 1-6.

[18] J. Peralta, H. Saad, S. Dennetiere, J. Mahseredjian and S. Nguefeu, "Detailed and averaged models for a 401-level MMC-HVDC system," *IEEE Trans. Power Delivery*, vol. 27, no. 3, July 2012, pp. 1501-1508.

[19] Temesgen M. Haileselassie, "Control, Dynamics and Operation of Multi-Terminal VSC-HVDC Transmission Systems," PhD Thesis, NTNU 2012.

[20] Lidong Zhang, "Modeling and control of VSC-HVDC links connected to weak AC systems," PhD Thesis, KTH Royal Institute of Technlogy, 2010.